Pergamon

Int. J. Heat Mass Transfer. Vol. 40, No. 6, pp. 1355–1364, 1997

0017–9310/97 $17.00 + 0.00

PII: S0017–9310(96)00201–3

Impingement cooling of a confined circular air jet

JUNG-YANG SAN, CHIH-HAO HUANG and MING-HONG SHU

Department of Mechanical Engineering, National Chung-Hsing University, 250 KuoKuang Road, Taichung, Taiwan, Republic of China

(*Received* 11 *September* 1995 *and in final form* 28 *May* 1996)

Abstract—A measurement of the local Nusselt number of a confined circular air jet vertically impinging on a flat plate is performed. The jet flow, after impingement, is constrained to exit in two opposite directions. Part of the impinging surface is maintained at a constant heat flux condition and the rest is adiabatic. The constant surface heat flux condition is modeled by conducting electricity through a thin stainless foil with a thickness of 0.01 mm. The heating foil was given constant heat flux values of 500, 1000, 1500 and 2000 W m^{-2}. Four diameters of the impinging jet 3, 4, 6 and 9 mm are considered individually. The jet Reynolds number is in the range of 30,000–67,000. The H/d is 2.0. The recirculation and mixing effect on the heat transfer is investigated by varying the jet diameter, surface heat flux, Reynolds number and surface heating width. The correlations of the local Nusselt number and the jet-to-adiabatic wall temperature difference are obtained. Copyright © 1996 Elsevier Science Ltd.

1. INTRODUCTION

Impingement cooling is an effective way to generate a high cooling rate in many engineering applications. In steel or glass industry impinging jets are used to cool down the products after rolling. In gas turbine engines impinging jets are applied to the cooling of turbine blades or vanes. In laser or plasma cutting processes, the application of jet impingement cooling can reduce thermal deformation of products. Besides the above applications, impinging jets are also adopted to enhance industrial drying processes or electronic cooling.

Jambunathan *et al.* [1] did a detailed survey on the impingement cooling of a single air jet. They concluded that the simplest correlations for local convective heat transfer coefficient is a function of the Reynolds number, H/d, x/d and the Prandtl number. Bouchez and Goldstein [2] investigated the impingement cooling of a circular jet with/without a cross flow. It was found that as the jet-to-cross flow mass flux ratio decreases within a moderate range, the stagnation point will be deflected by the cross flow; consequently the stagnation point moves downstream. As the jet-to-cross flow mass flux ratio increases, a recirculation and mixing zone was visualized. In the experiment the surface heat flux was in the range of 320–1200 W m^{-2} and the jet spacing-to-diameter ratio was arranged to be 6 and 12 respectively. Since the surface heat flux is low and the jet spacing-to-diameter ratio is high, the convective heat transfer coefficient was found to be almost irrelevant to the surface heat flux.

Sparrow *et al.* [3] also investigated the heat transfer of a vertical confined impinging circular jet with a cross flow. The velocity of the cross flow was fixed at 12 m s^{-1} and the jet mean velocity was varied. It was found that the convective heat transfer coefficient with jet impingement can be ten times higher than that without an impinging jet. In the result the convective heat transfer coefficient was represented as a function of the jet-to-cross flow mass flux ratio, the location and the jet spacing-to-diameter ratio. For a mass flux ratio more than eight, an optimum jet spacing-to-diameter ratio was clearly observed. The optimum ratio corresponds to a peak value of the convective heat transfer coefficient. For the condition of jet spacing-to-diameter ratio less than the optimum value, the jet is in a potential core. If so, the intensity of turbulence intensity decreases as the jet spacing-to-diameter ratio decreases. Thus the peak convective heat transfer coefficient descends. Alternatively as the jet spacing-to-diameter ratio is greater than the optimum value, the peak convective heat transfer coefficient also decreases due to a strong mixing effect.

Goldstein and Behbahani [4] performed an experiment on a confined circular jet, with and without a cross flow. The jet temperature was controlled to equal the temperature of the cross flow and the room temperature. They concluded that at large jet-to-plate spacing, the cross flow diminishes the convective heat transfer coefficient; at small jet-to-plate spacing, the cross flow can increase the peak convective heat transfer coefficient. This increase is attributed to an increase in the jet centerline intensity from the mixing of the cross-flow stream. Goldstein *et al.* [5] summarized the previous works on jet impingement. A recovery factor is defined to express the nondimensional form of the adiabatic wall temperature. In this work the recovery

NOMENCLATURE

a_i, b_i, c_i	coefficients of regression analysis
d	jet hole diameter [mm]
d_0	reference jet hole diameter, 1 mm
d^*	diameter ratio, d/d_0
f_1, f_2, f_3	functions
H	distance from jet exit to impingement plate [mm]
h	convective heat transfer coefficient, $q/(T_w - T_{aw})$ [W m^{-2} °C^{-1}]
k	thermal conductivity of air [W m^{-1} °C^{-1}]
k_i	coefficients of regression analysis
Nu	local Nusselt number, hd/k
Nu_{sg}	stagnation Nusselt number, hd/k
q	surface heat flux [W m^{-2}]
Q	volumetric flowrate, [m^3 s^{-1}]
Re	Reynolds number, $4Q/\pi\nu d$
T_{aw}	adiabatic wall temperature [°C]
T_j	jet total temperature [°C]
T_w	local wall temperature [°C]
w	width of heated area [m]
x, y	coordinates [m].

Greek symbols

α, λ	power of Reynolds number in regression analysis
β_i, γ_{ij}	coefficients in regression analysis
Δ	difference
ν	kinematic viscosity [m^2 s^{-1}].

factor is found to be independent of the jet Reynolds number and is dependent on the jet spacing-to-diameter ratio.

Goldstein *et al.* [6] investigated the effect of entrainment on the heat transfer to an unconfined heated circular air jet impinging on a flat plate. For the considered range of jet Reynolds number and jet total temperature, they found that the Nusselt number and heat transfer effectiveness are not affected by the temperature difference between the ambient air and the jet. Besides the direct measurement of the surface temperature, a new technique, by measuring the amount of sublimation of naphthalene, was developed, for the evaluation of the heat transfer coefficient on the jet impingement surface [7]. This sublimation technique can be applied to almost any cooling surface with a complex geometry. An analogy between the heat transfer and mass transfer is adopted in the technique. Sparrow *et al.* [7] applied this method to measure the mass transfer coefficient of a circular jet normally impinging on a flat plate. It was found that the dimensionless mass transfer coefficient varied with the 0.8 power of the jet Reynolds number.

An optical technique developed by Goldstein and Timmers [8] and Goldstein and Franchett [9] was used in measuring the heat transfer of an impinging jet with different inclined angles. A temperature-sensitive liquid crystal was sandwiched between a thin metallic-foil heater and a specially designed liquid bath. Thus the thermal condition on the impinging plate falls between constant heat flux and constant surface temperature. In these works the isothermal lines on the impinging plate were observed and the contours of constant Nusselt number were obtained.

The heat transfer of an unconfined jet impinging on a flat plate with low Reynolds number and jet spacing-to-diameter ratio was investigated by Huang and El-Genk [10]. In this work the average Nusselt number was found to be proportional to $Re^{0.76}$. The measurement of the heat transfer of an unconfined impinging jet with the jet spacing-to-diameter ratio less than 1.0 was performed by Lytle and Webb [11]. For a jet spacing less than 0.25 times the jet diameter the effect of fluid acceleration between the nozzle wall and impingement plate was seen; this results in a clear observation of the secondary maxima in the Nusselt number.

Recently Huber and Vistanta [12] investigated the effect of jet–jet spacing on convective heat transfer to a confined impinging jet array. A thermochromatic liquid crystal technique was used to visualize and measure the isotherms on the impingement plate. They found that, for a high separation distance between the jet and impingement plate, the adjacent jet interference before impingement will cause significant degradation of the convective heat transfer coefficient. The effect of a spent air arrangement on the heat transfer was also investigated. It was found that the spent air results in a heat transfer enhancement by minimizing adjacent jet interference in the wall jet region.

The diameter dependency on the Nusselt number for a jet impinging on an isothermal plate was investigated by Hollworth and Gero [13]. For cases with values of H/d greater than 10.0, the jet diameter showed no effect on the Nusselt number. Due to the limitation of the measurement, this experiment did not verify this point for cases with a lower value of H/d. Stevens and Webb [14] investigated the local heat transfer coefficients for a free liquid jet impinging normally on a uniform heat flux surface. The ratio of mean jet velocity to jet diameter was proposed, in the correlation, to vanish the nozzle size dependency.

The local heat transfer from a small heat source to a normally impinging, confined and submerged liquid jet was experimentally investigated by Garimella and Rice [15]. The nozzle-to-heat source spacing, jet Reynolds number and nozzle diameter, were explored as

variables. The results indicate that at the stagnation point, for a given Reynolds number and nozzle-to-heat source spacing, the smaller nozzle produces a lower Nusselt number. The correlations for the stagnation point and area-averaged heat transfer coefficients were expressed in terms of jet Reynolds number, fluid Prandtl number, nozzle-to-heat source spacing and nozzle aspect ratio. In the work a flow visualization of the jet impingement was included. The pathline of a secondary recirculation zone was clearly illustrated.

In this work the local Nusselt number of a confined circular air jet vertically impinging on a flat plate is investigated. The aspect ratio of the jet orifice is 1.0. Four different jet hole diameters, namely 3, 4, 6 and 9 mm are considered individually. The Reynolds number, the surface heating width and the surface heat flux, on the heated area are the variables in the measurement. It is intended to realize the effect of the jet hole diameter on the heat transfer of a confined jet impingement, for various operating conditions.

2. LOCAL NUSSELT NUMBER

In this work the convective heat transfer coefficient, h, is defined as the local surface heat flux, q divided by $(T_w - T_{aw})$. Both T_w and T_{aw} are measured locally. In a well-insulated channel the temperature difference, $(T_j - T_{aw})$, is only dependent on the jet Reynolds number and the jet hold diameter. In solving an engineering problem both the valves of h and $(T_j - T_{aw})$ need to be known.

The local heat transfer coefficient, h, for the impingement of a confined circular air jet on a partly constant heat-flux plate (Fig. 1), is a function of several variables. Combined with k and d, a local Nusselt number, Nu, is formed. Thus the local Nusselt number in the flow direction, for a specific jet diameter and orifice aspect ratio, is also a function of several variables and it can be expressed as follows:

$$Nu = Nu(H/d, x/d, Re, q, w/d). \quad (1)$$

In this work the jet spacing-to-diameter ratio is fixed at 2.0. The jet diameter and the other parameters in equation (1) will be treated as the variables in the measurement.

3. APPARATUS AND PROCEDURE

The experimental setup for the measurement is shown in Fig. 2. It can mainly be divided into two parts. One is related to the high pressure supplied air, the other is related to the sensor signal lines. The high pressure air is supplied by a large reciprocating air compressor. The air pressure in the compressor tank is in the range of 5–6 kg cm^{-2}. A pressure regulator is installed at the exit of the compressor to control the exit air pressure. The high pressure supplied air needs dehydration and oil removal before used for impinge-

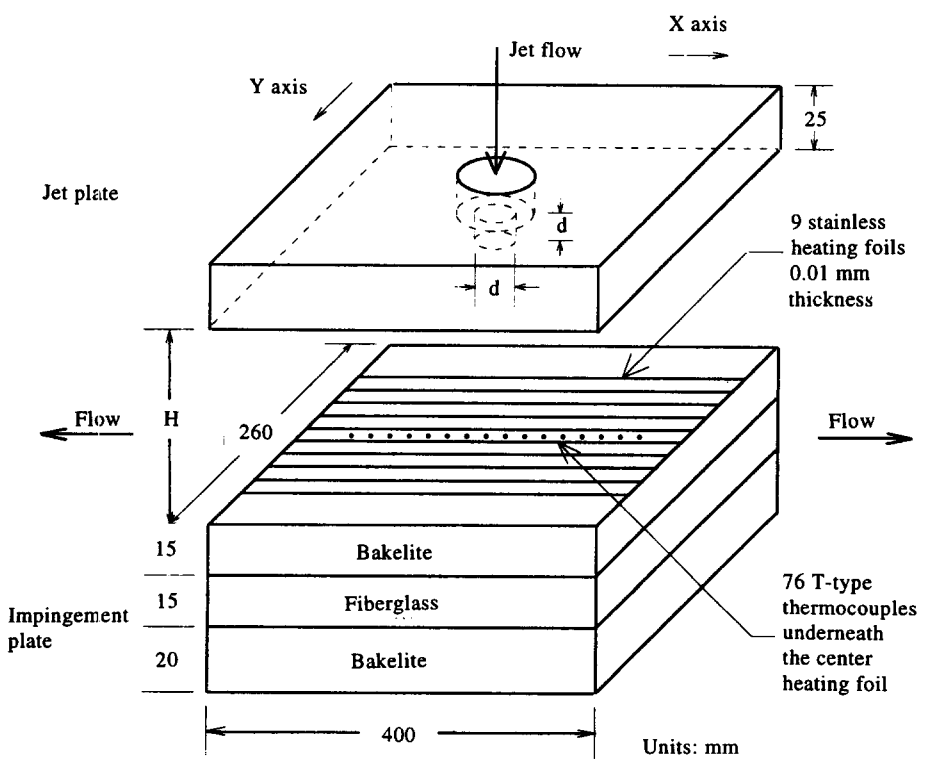

Fig. 1. Impingement and jet plates.

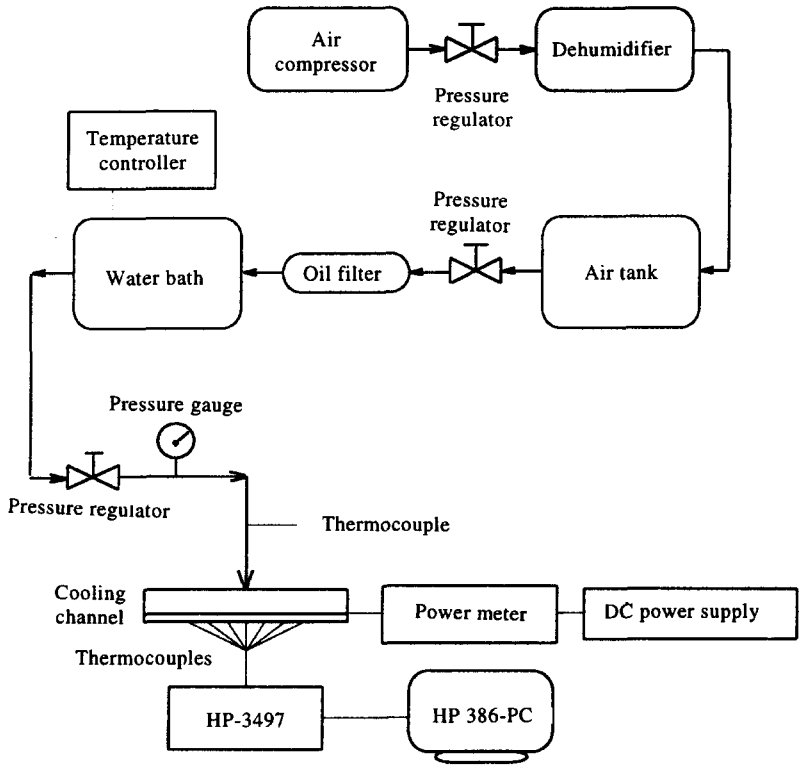

Fig. 2. Experimental apparatus.

ment cooling. This is done by installing a vapor compression type dehumidifier and a column filled with active carbon particles in the supplied air line. The dehumidified air is stored in a large surge tank in which the pressure is maintained at 3 kg cm^{-2}. The function of the surge tank is to diminish the pressure fluctuation due to the on-off cycling of the air compressor. A pressure regulator is installed at the exit of the tank to control the exit air pressure. In order to reduce the temperature variation of the supplied air, a temperature-controlled water bath embedded with a heat exchanger coil is installed. In doing so, the air temperature can be regulated simply by controlling the water temperature. In this work the temperature variation of the water and air is controlled within 0.1°C.

The geometry of the jet plate and the impingement plate is shown in Fig. 1. The width of the jet and impingement plates is 260 mm and the length, 400 mm. The air in the channel is restricted to flow only in the two opposite directions, as shown in Fig. 1. Nine 0.01 mm thickness stainless heating foils are attached to the impingement plate. The adhesive is nonconductive. The width of the heating foil is 12.5 mm and the length, 400 mm. The discontinuities between the heating foils are filled with a silicone material to produce a smooth impingement surface. The joint between the heating foil and the electricity wire is carefully soldered to access a negligible voltage drop. The resistance of every heating foil is carefully examined to ensure the heating is uniform on the surface. High pressure air passes through the jet hole directly impinging on the middle heating foil.

The middle heating foil is embedded with 76 T-type thermocouples. The diameter of the thermocouples is 0.1 mm and the bead is less than 0.25 mm. Besides the adhesive layer, a thermally well-conductive paste is applied between the heating foil and the thermocouple beads. The paste is also dielectric. This insures that the signal of the thermocouples is not disturbed by the electricity on the heating foil. A d.c. electric current is conducted to heat the foil with a uniform heat generation rate. The supplied power to the heating foils is measured by an accurate digital power meter. The spacing of any two neighboring thermocouples is 3 mm. The measurement was conducted in a room with air conditioning. In such an arrangement the room temperature can be controlled within a deviation of 1.5°C from the jet total temperature.

In this experiment the jet plate can be moved in the x- and y-directions individually by adjusting two screws. The jet plate is positioned by using two linear photoelectronic scales, which provide a smallest readout of 0.001 mm. In the present work, only one thermocouple is used throughout the entire measurement, which has the advantage of consistency. Thus, the inaccuracy of the temperature measurement can be minimized. The heating foil is stuck on a Bakelite plate which has a thickness of 15 mm. Below it there is a 15 mm fiberglass insulation. The bottom of the impingement plate is a 20 mm thickness Bakelite plate to support the insulation. The jet plate is made of

acrylic. To reduce the heat loss from the jet plate, it is covered with a 20 mm thickness PS foam, which ensures that the impingement plate and the jet plate are well-insulated. During the operation a long time period is required for the system to reach a thermally steady-state condition. In this work a waiting period of three hours is set at the beginning of every adiabatic or heated wall measurement, after which, for every point measurement there is a waiting period of 10–15 minutes. The temperature of the measured point is recorded by a HP-3497 data acquisition system. The obtained data are analyzed by using a 386 personal computer.

A turbine flowmeter (EG & G Co.) is installed upstream of the high pressure supplied air. To avoid a continuous long period operation of the turbine flowmeter, the turbine flowmeter is only used to calibrate a pressure gauge for every measured Reynolds number. Once the calibration between the pressure and Reynolds number is done, the valves in front and after the turbine flowmeter will be closed. The flow is then bypassed in a tube directly to the pressure gauge and jet plate.

4. ERROR ANALYSIS

The uncertainty in the measurement can be separated into two parts. The first is from the mass flowrate; the second is from the convective heat transfer coefficient. The former is due to the inaccuracy of the turbine flowmeter. According to the manufacturer's supplied data a 1% error on the measurement is assured. The inaccuracy of the latter is attributed to the following reasons.

Heat flux error:
- radiation loss, 3.1%;
- nonuniformity of the heating foil, less than 4.4%;
- lateral solid heat conduction, 2.0%;
- heat loss through insulation, 0.9%.

Temperature error:
- thermal resistance of epoxy resin, less than 0.01K;
- inaccuracy due to thermocouple, 35 ± 0.2°C.

In the experiment a high accuracy of the temperature measurement is demanded. In the evaluation of the convective heat transfer coefficient only the difference of the adiabatic wall temperature and heated wall temperature is needed. In this work the same thermocouple is used to measure the two temperatures, thus the inaccuracy of the temperature measurement is reduced. Neglecting the error in the temperature measurement the uncertainty in Nusselt number of this experiment is 5.81%.

5. RESULTS

Most of the previous works on impingement heat transfer are concerned with unconfined jets. Thus it is difficult, simply by comparing the measured data, to confirm the accuracy of the present work. For this reason, in this work a minor change of the present setup is done for the measurement of an unconfined jet. Two jet diameters are considered. One is 3 mm and the other is 10 mm. Figure 3 shows a comparison of a set of the present data with that in Goldstein and Franchett's work [9]. In Goldstein and Franchett's work only the jet diameter of 10 mm was considered. Both the above measurements are based on a similar operating condition and they are mainly related to the heat transfer of an unconfined air jet. For the case with the jet diameter of 10 mm, the result in Fig. 3 shows a good agreement between the present work and Goldstein and Franchett's work [9]. Figure 3 also shows the effect of the jet diameter on the Nusselt number. For a smaller jet diameter, the Nusselt number tends to be smaller.

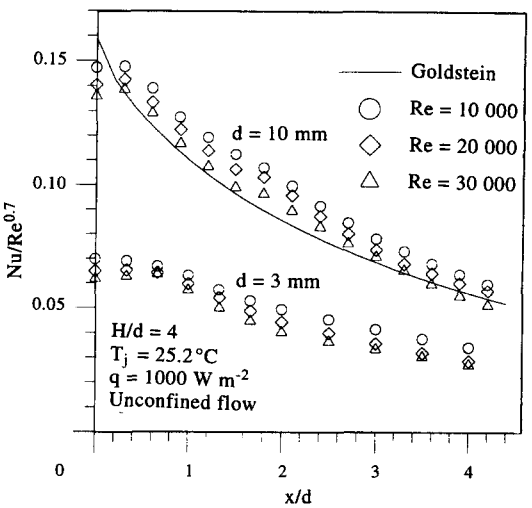

Fig. 3. Comparison of the results for an unconfined jet flow.

Figure 4 shows the effect of surface heat flux on the Nusselt number for various jet Reynolds number. The

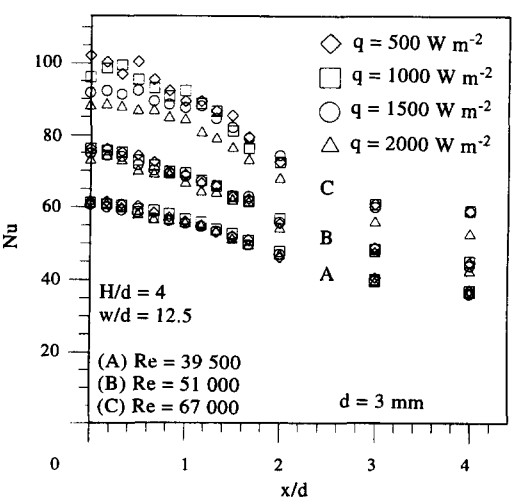

Fig. 4. Effect of jet Reynolds number and heat flux on local Nusselt number.

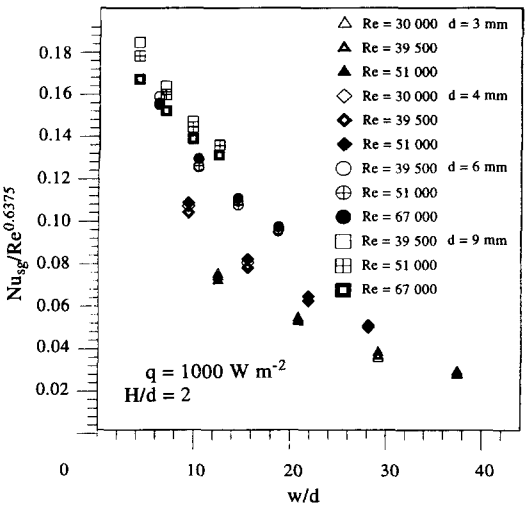

Fig. 5. Local Nusselt number at stagnation point.

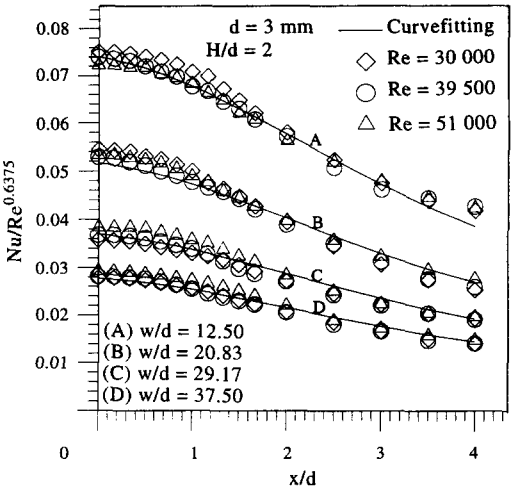

Fig. 6. Local Nusselt number for jet diameter of 3 mm.

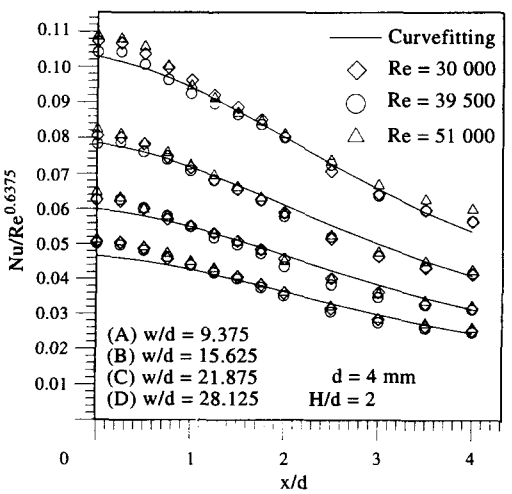

Fig. 7. Local Nusselt number for jet diameter of 4 mm.

recirculation zone for a confined jet impingement was clearly illustrated by Garimella and Rice [15]. For the case with a lower jet Reynolds number, the flow recirculation and mixing near the stagnation point is weaker. Thus the generated energy on the heating foils can be easily removed. For an increase of the surface heat flux, without having the flow recirculation, there will be a proportional increase of the heated wall-to-adiabatic wall temperature difference. Hence, the local convective heat transfer coefficient and Nusselt number remains almost unchanged. For the case with a higher jet Reynolds number, the flow recirculation and mixing is stronger. This results in the downstream heated air recirculated to the upstream; due to the mixing process a higher fluid temperature near the impingement plate is formed. Thus, the jet cooling effect is degraded and the local Nusselt number decreases. Generally speaking, the effect of surface heat flux on the local Nusselt number is significant only when the jet Reynolds number is high.

Figure 5 presents the effect of the heating width-to-jet diameter ratio, w/d, on the stagnation Nusselt number for four different jet diameters. There are in total, nine heating foils used in the experiment; by disconnecting electricity from the outer symmetric heating foils, the heating width can be changed. In this work, part of the impinging surface is maintained at the constant heat flux condition and the rest is adiabatic. The stagnation Nusselt number is found to be proportional to $Re^{0.6375}$. The heating width-to-jet diameter ratio appears to be an important factor affecting the stagnation Nusselt number. As the heating width increases, the air temperature in the channel also tends to increase. Due to the strong mixing and recirculation effect the jet temperature also increases. This results in the descent of the stagnation Nusselt number. But as the value of w/d exceeds 40, the stagnation Nusselt number is obviously not very dependent on the w/d.

Figure 5 also shows that the jet hole diameter strongly affects the stagnation Nusselt number. But as the jet hole diameter exceeds 6 mm, the effect of the jet hold diameter on the stagnation Nusselt number tends to the minor. In other words, at that moment the convective heat transfer coefficient will decrease almost at the same rate as the increase of the jet diameter. For the same value of the Reynolds number, a higher value of the jet diameter implies a lower value of the jet velocity. The strength of the mixing and recirculation is related to the jet velocity. For a larger jet diameter the mixing and recirculation is weaker. Thus the effect of the jet diameter on the stagnation Nusselt number is minor.

Figures 6–9 show the distribution of local Nusselt number individually for the jet hole diameters of 3, 4, 6 and 9 mm. In the diagrams $Nu/Re^{0.6375}$ is represented as a function of x/d and w/d. The result shows that the w/d is a strong function affecting the distribution of the local Nusselt number. Also for the case with a large jet hold diameter, there seems to be an inflection

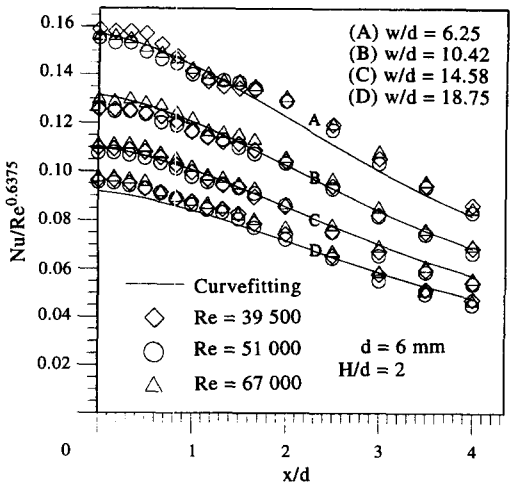

Fig. 8. Local Nusselt number for jet diameter of 6 mm.

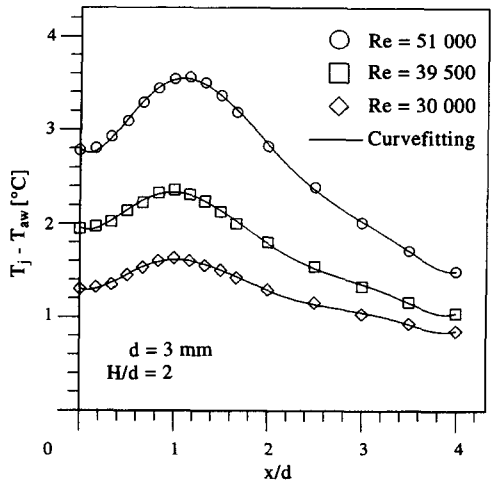

Fig. 10. Local temperature difference for jet diameter of 3 mm.

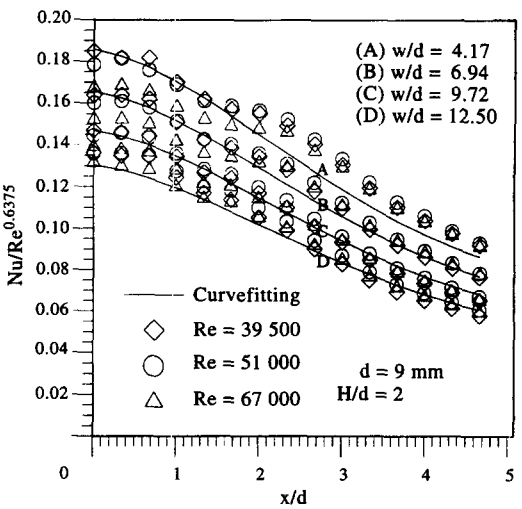

Fig. 9. Local Nusselt number for jet diameter of 9 mm.

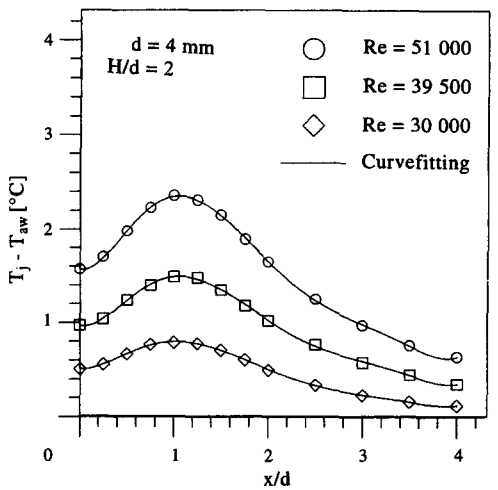

Fig. 11. Local temperature difference for jet diameter of 4 mm.

point of the local Nusselt number occurring at the value of x/d between 1.0 and 2.0, which is attributed to the transition point between the impingement region and the wall jet region [15]. This phenomenon will be discussed in the following paragraph.

Figures 10–13 show the distribution of jet-to-adiabatic wall temperature difference, respectively, for the jet hole diameters of 3, 4, 6 and 9 mm. The result shows that the temperature difference decreases as the jet hole diameter increases. In Figures 10–13 there is a maximum temperature difference for the value of x/d between 1.0 and 2.0. The maximum temperature difference represents the minimum of the adiabatic wall temperature on the impingement plate. This phenomenon is also due to the occurrence of the transition point. At the transition point the jet flow is changed from the impingement region to the wall jet region. Before the transition point the flow accelerates, thus the flow temperature drops. This also results in the drops of the local adiabatic wall temperature and consequently the temperature difference,

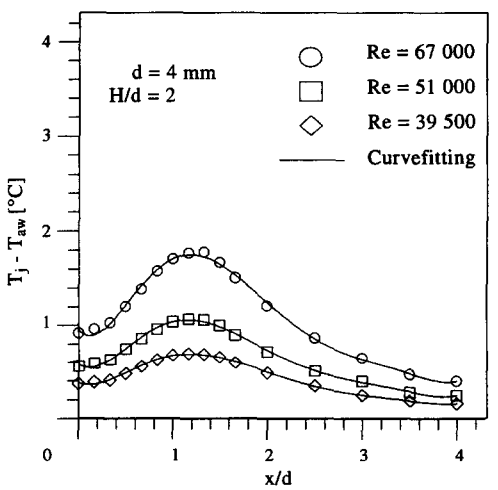

Fig. 12. Local temperature difference for jet diameter of 6 mm.

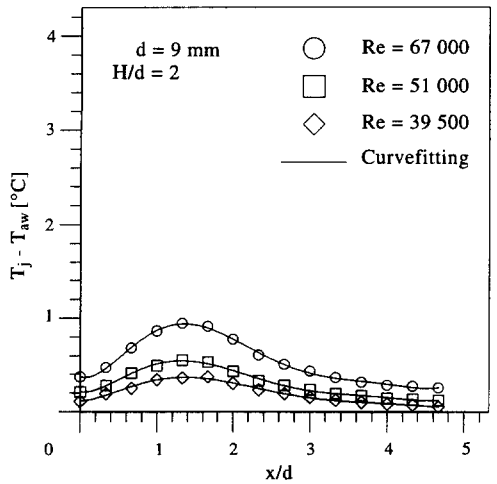

Fig. 13. Local temperature difference for jet diameter for 9 mm.

$(T_j - T_{aw})$ rises. After passing through the transition point, the flow is in the wall jet region. The flow starts to decelerate. Thus the adiabatic wall temperature rises and the temperature difference drops. In the results it also indicates that the location of the maximum temperature difference varies slightly with the jet diameter. For a larger jet diameter, with the same jet Reynolds number, the jet exit velocity is relatively slower. Thus the jet is not as convergent as that with a smaller jet diameter. This results in a larger value of x/d for the occurrence of the transition point with a larger jet diameter.

In Figures 6–13 the solid lines represent the curvefitting results. From the comparison, there is only a small deviation between the measured data and curvefitting results. Thus the equations developed in the regression analysis provide a good accuracy for engineering applications.

6. REGRESSION ANALYSIS

The local Nusselt number of the confined jet impingement heat transfer is a function of many variables. A regression analysis is carried out to reduce the measured data. In a practical application, the difference between the jet total temperature and adiabatic wall temperature also has to be known. In this work the distribution of the temperature difference is expressed as a function of the Reynolds number and x/d for each jet diameter. The stagnation temperature difference is correlated as a function of the Reynolds number and jet diameter.

Local Nusselt number

The Nusselt number is expressed as follows:

$$\ln\left(\frac{Nu}{Re^{\alpha}}\right) = f_1\left(\frac{x}{d}\right) + f_2\left(\frac{w}{d}\right) + f_3\left(\frac{d}{d_0}\right) \qquad (2)$$

in which

Table 1. Coefficients for regression analysis of Nusselt number

	$i=1$	$i=2$	$i=3$	$i=4$
a_i	−0.042035	−0.051099	0.004587	0.000154
b_i	−0.038785	−0.000332	0.000008	—
c_i	−2.757427	0.232741	0.001383	−0.001325

$$f_1 = \sum_{i=1}^{4} a_i \left(\frac{x}{d}\right)^i$$

$$f_2 = \sum_{i=1}^{3} b_i \left(\frac{w}{d}\right)^i$$

$$f_3 = \sum_{i=1}^{4} c_i \left(\frac{d}{d_0}\right)^{i-1}.$$

In equation (2) α is found to be 0.63745 and the corresponding coefficients a_i, b_i and c_i are listed in Table 1. The above equation is valid for Reynolds numbers between 30 000 and 67 000. The range of w/d is valid between 4.0 and 37.5. The diameter is valid between 3 and 9 mm. The value of x/d is valid between 0 and 4.0. The mean value of the error is 3.2% and the maximum error is 11.085%. In the work the jet hole diameter is scaled by dividing a reference jet hole diameter, d_0. The reference jet hole diameter is selected to be 1 mm. The reference jet hole diameter is an arbitrarily selected length scale which is used to non-dimensionalize the jet hole diameter. Hence the ratio, d/d_0, only represents a comparison, it is itself not a physical parameter. In the work the effect of the size of the jet plate (width and length) on the Nusselt number has not been investigated. The size of jet plate might influence the flow recirculation in the channel and thus the mixing of the upstream colder air with the downstream hotter air. It is suspected that the width and length of the jet plate are the length scales which should be used to replace the reference jet hold diameter. But this viewpoint needs to be further verified by experimental work.

Distribution of temperature difference

The temperature difference is expressed as follows:

$$T_j - T_{aw} = \sum_{i=0}^{6} \beta_i \left(\frac{x}{d}\right)^i \qquad (3)$$

in which

$$\beta_i = \sum_{j=0}^{2} \gamma_{i,j} Re^j.$$

The coefficients in equation (3) are listed in Table 2. It is valid for Reynolds numbers between 30 000 and 67 000. The range of w/d is valid between 4.0 and 37.5. The diameter is valid between 3 and 9 mm. The value of x/d is valid between 0 and 4.0. The mean

Table 2. Coefficients for regression analysis of temperature difference

d	$\gamma_{i,j}$	$j=0$	$j=1$	$j=2$
$d=3$ mm	$i=0$	-0.5174000	5.468730×10^{-5}	2.010920×10^{-1}
	$i=1$	-0.7507930	3.662650×10^{-5}	-7.684340×10^{-1}
	$i=2$	4.2890800	-1.832260×10^{-4}	4.004030×10^{-0}
	$i=3$	-2.5992900	7.429060×10^{-5}	-2.688470×10^{-0}
	$i=4$	0.4831000	8.445970×10^{-6}	6.201790×10^{-1}
	$i=5$	0.0091233	-8.369260×10^{-6}	-3.214850×10^{-1}
	$i=6$	-0.0074288	1.059610×10^{-6}	-3.432870×10^{-1}
$d=4$mm	$i=0$	-0.7310270	3.591970×10^{-5}	1.809590×10^{-1}
	$i=1$	1.9551600	-1.007150×10^{-4}	1.110830×10^{-0}
	$i=2$	-6.9921700	3.731760×10^{-4}	-3.002290×10^{-0}
	$i=3$	7.0588200	-3.802020×10^{-4}	2.821690×10^{-0}
	$i=4$	-3.1474700	1.694190×10^{-4}	-1.245580×10^{-0}
	$i=5$	0.6496130	-3.483620×10^{-5}	2.579720×10^{-1}
	$i=6$	-0.0505310	2.697850×10^{-6}	-2.012010×10^{-1}
$d=6$ mm	$i=0$	0.1564610	-3.223770×10^{-6}	2.253540×10^{-1}
	$i=1$	-0.2538940	1.075880×10^{-5}	-3.498560×10^{-1}
	$i=2$	-0.7076840	3.342960×10^{-5}	9.025880×10^{-1}
	$i=3$	2.0540300	-8.767070×10^{-5}	-4.152070×10^{-1}
	$i=4$	-1.3993560	5.796804×10^{-5}	-2.202783×10^{-1}
	$i=5$	0.3687560	-1.505450×10^{-5}	4.036620×10^{-1}
	$i=6$	-0.0338590	1.370890×10^{-6}	-5.453070×10^{-1}
$d=9$ mm	$i=0$	-0.1118230	3.565792×10^{-6}	5.456585×10^{-1}
	$i=1$	0.6182650	-1.760473×10^{-5}	7.447498×10^{-1}
	$i=2$	-0.6355470	1.832680×10^{-5}	3.279085×10^{-1}
	$i=3$	0.7738077	-2.639213×10^{-5}	-2.142404×10^{-1}
	$i=4$	-0.4306971	1.537750×10^{-5}	2.899523×10^{-1}
	$i=5$	0.0988944	-3.579812×10^{-6}	4.056140×10^{-1}
	$i=6$	-0.0079622	2.896273×10^{-7}	-8.159726×10^{-1}

Table 3. Coefficients for regression analysis of temperature difference at the stagnation point.

	k_i
$i=1$	-12.40872369
$i=2$	-4.31917039
$i=3$	0.89268942
$i=4$	-0.0776337
$i=5$	0.00024554
$i=6$	0.00020059

value of the error is 2.55% and the maximum error is 8.4%.

Stagnation temperature difference

The temperature difference at the stagnation point is expressed as follows:

$$\ln\left(\frac{T_i - T_{aw}}{Re^{\lambda}}\right) = \sum_{i=1}^{6} k_i \left(\frac{d}{d_0}\right)^{i-1}. \quad (4)$$

In equation (4) λ is found to be 1.89254 and the coefficients are listed in Table 3. The mean value of the error is 6.588% and the maximum error is 14.158%.

7. CONCLUSIONS

The correlations of the Nusselt number and jet-to-adiabatic wall temperature difference are obtained for the case with the jet spacing-to-diameter ratio of 2.0. The correlations are based on the measured data in the range of $30\,000 \leqslant Re \leqslant 67\,000$, $3 \leqslant d/d_0 \leqslant 9$, $0 \leqslant x/d \leqslant 4.0$ and $4.17 \leqslant w/d \leqslant 37.5$.

Similar to the result of an unconfined impinging jet, the Nusselt number of the confined jet is found to be proportional to the 0.6375 power of the Reynolds number. It is also found that the jet hole diameter is a strong factor affecting the Nusselt number. This implies that for the same Reynolds number, the case with a smaller jet hole diameter will have a lower value of the Nusselt number. But for a jet hole diameter greater than 6 mm, the influence of the jet hole diameter on the Nusselt number will tend to decrease.

The transition of the confined jet from the impingement region to the wall jet region can be observed from the local surface temperature distribution. It is found that the transition occurs at the value of x/d near 1.0. For the case with a larger jet hole diameter the location of the transition will take place further downstream. Due to the mixing in the shear layer and flow recirculation around the stagnation point, the surface heat flux may become a factor slightly affecting the Nusselt number for confined jet impingement heat transfer. The higher the Reynolds number, the greater the effect of surface heat flux on the Nusselt number. In this work the influence of the effect is not very significant.

The surface heating width on the impingement plate

is also a factor dominating the Nusselt number. For a specific jet hole diameter, the greater the surface heating width, the lower the Nusselt number. This phenomenon is due to the flow recirculation and mixing. But as the surface heating width increases beyond 40 times the jet hole diameter, the Nusselt number at the stagnation point tends to be independent of the surface heating width.

REFERENCES

1. Jambunathan, K., Lai, E., Moss, M. A. and Button, B. L., A review of heat transfer data for single circular jet impingement. *International Journal of Heat Fluid Flow*, 1992, **13,** 106–115.
2. Bouchez, J. P. and Goldstein, R. J., Impingement cooling from a circular jet in a cross flow. *International Journal of Heat and Mass Transfer*, 1975, **18,** 719–730.
3. Sparrow, E. M., Goldstein, R. J. and Rouf, M. A., Effect of nozzle surface separation distance on impingement heat transfer for a jet in a crossflow. *ASME Journal of Heat Transfer*, 1975, **97,** 528–533.
4. Goldstein, R. J. and Behbahani, A. I., Impingement of a circular jet with and without cross flow. *International Journal of Heat and Mass Transfer*, 1982, **25,** 1377–1382.
5. Goldstein, R. J., Behbahani, A. I. and Heppelmann, K. K., Streamwise distribution of the recovery factor and the local heat transfer coefficient to an impinging circular air jet. *International Journal of Heat and Mass Transfer*, 1986, **29,** 1227–1235.
6. Goldstein, R. J., Sobolik, K. A. and Seol, W. S., Effect of entrainment on the heat transfer to a heated circular air jet impinging on a flat surface. *ASME Journal of Heat Transfer*, 1990, **112,** 608–611.
7. Sparrow, E. M., Xu, Z. X. and Azevedo, L. F. A., Heat (mass) transfer for circular jet impingement on a confined disk with annular collection of the spent air. *ASME Journal of Heat Transfer*, 1987, **109,** 329–335.
8. Goldstein, R. J. and Timmers, J. F., Visualization of heat transfer from arrays of impinging jets. *International Journal of Heat and Mass Transfer*, 1982, **25,** 1857–1868.
9. Goldstein, R. J. and Franchett, M. E., Heat transfer from a flat surface to an oblique impinging jet. *ASME Journal of Heat Transfer*, 1988, **110,** 84–90.
10. Huang, L. and El-Genk, M. S., Heat transfer of an impinging jet on a flat surface. *International Journal of Heat and Mass Transfer*, 1994, **37,** 1915–1923.
11. Lytle, D. and Webb, B. W., Air jet impingement heat transfer at low nozzle-plate spacing. *International Journal of Heat and Mass Transfer*, 1994, **37,** 1687–1697.
12. Huber, A. M. and Viskanta, R., Effect of jet–jet spacing on convective heat transfer to confined, impinging arrays of axisymmetric air jets. *International Journal of Heat and Mass Transfer*, 1994, **37,** 2859–2869.
13. Hollworth, B. R. and Gero, L. R., Entrainment effects on impingement heat transfer: part II—local heat transfer measurements. *ASME Journal of Heat Transfer*, 1985, **107,** 910–915.
14. Stevens, J. and Webb, B. W., Local heat transfer coefficients under an axisymmetric, single-phase liquid jet. *ASME Journal of Heat Transfer*, 1991, **113,** 71–78.
15. Garimella, S. V. and Rice, R. A., Confined and submerged liquid jet impingement heat transfer. *ASME Journal of Heat Transfer*, 1995, **117,** 871–877.